



Research paper

 Δ^5 -Cholenoyl-amino acids as selective and orally available antagonists of the Eph–ephrin system

Riccardo Castelli ^a, Massimiliano Tognolini ^{a, **}, Federica Vacondio ^a, Matteo Incerti ^a, Daniele Pala ^a, Donatella Callegari ^a, Simona Bertoni ^a, Carmine Giorgio ^a, Iftiin Hassan-Mohamed ^a, Ilaria Zanotti ^a, Antonella Bugatti ^b, Marco Rusnati ^b, Claudio Festuccia ^c, Silvia Rivara ^a, Elisabetta Barocelli ^a, Marco Mor ^a, Alessio Lodola ^{a, *}

^a Dipartimento di Farmacia, Università degli Studi di Parma, Parco Area delle Scienze 27/A, 43124, Parma, Italy

^b Dipartimento di Medicina Molecolare e Traslazionale, Università degli Studi di Brescia, Viale Europa 11, 25123, Brescia, Italy

^c Dipartimento di Scienze Cliniche Applicate e Biotecnologiche, Università degli Studi dell'Aquila, Via Vetoio, Coppito 2, 67100, L'Aquila, Italy

ARTICLE INFO

Article history:

Received 29 April 2015

Received in revised form

24 August 2015

Accepted 25 August 2015

Available online 29 August 2015

Keywords:

Protein–protein interaction inhibitors

Eph–ephrin antagonists

EphA2

Anti-angiogenic agents

Oral bioavailability

Bile acids

ABSTRACT

The Eph receptor–ephrin system is an emerging target for the development of novel anti-angiogenic therapies. Research programs aimed at developing small-molecule antagonists of the Eph receptors are still in their initial stage as available compounds suffer from pharmacological drawbacks, limiting their application *in vitro* and *in vivo*. In the present work, we report the design, synthesis and evaluation of structure–activity relationships of a class of Δ^5 -cholenoyl-amino acid conjugates as Eph–ephrin antagonists. As a major achievement of our exploration, we identified *N*-(3 β -hydroxy- Δ^5 -cholen-24-oyl)-L-tryptophan (UniPR1331) as the first small molecule antagonist of the Eph–ephrin system effective as an anti-angiogenic agent in endothelial cells, bioavailable in mice by the oral route and devoid of biological activity on G protein-coupled and nuclear receptors targeted by bile acid derivatives.

© 2015 Elsevier Masson SAS. All rights reserved.

1. Introduction

The erythropoietin-producing hepatocellular carcinoma (Eph) receptors constitute the largest family of receptor tyrosine kinases, composed of fourteen receptor subtypes divided in the A (EphA1–A8) and B (EphB1–EphB6) classes [1]. Together with their membrane-bound ligands, i.e. the ephrins, they represent a key cell–cell communication system essential both for the development of the embryos and the renewal of adult tissues [2]. The

Eph–ephrin system regulates the majority of the morphogenetic processes occurring during the embryonic development, whereas in the adult is predominantly involved in the maintenance of cellular architecture of various epithelial tissues [3]. Increasing evidence supports the notion that a few specific subtypes of Eph receptors, namely EphA2, EphB2 and EphB4, are involved in tumor and vascular functions during carcinogenesis [4]. In particular, the inhibition of EphA2 receptor with monoclonal antibodies [5] or recombinant proteins [6] has been shown to impair tumor angiogenesis in animal models [7], thus blocking the growth of solid tumors (i.e. pancreatic, breast and lung cancers), and to reduce the insurgence of peripheral metastasis. Furthermore, the EphA2 receptor has been exploited to deliver cytotoxic anticancer drugs into EphA2-expressing cancer cells, using peptides selectively targeting the EphA2 receptor [8]. From these premises, EphA2 emerges as a promising target for the development of antiangiogenic and antitumorogenic therapies [9].

Early efforts aimed at the discovery of agents targeting the Eph–ephrin system led to the identification of peptides of moderate size (i.e. composed by twelve residues) able to bind the

Abbreviations: EphA2, ephrin receptor A2; PPI, protein–protein interaction; HUVEC, human umbilical vein endothelial cell; FXR, farnesoid X receptor; TGR5, G protein-coupled bile acid receptor 1; PXR, pregnane-X receptor; ELISA, enzyme-linked immunosorbent assay; DMF, di-methyl formamide; DIPEA, di-isopropyl ethyl amine; TBTU, (O-(Benzotriazol-1-yl)-N,N,N',N'-tert-amethylurionium tetrafluoroborate).

* Corresponding author.

** Corresponding author. Dipartimento di Farmacia, Università degli Studi di Parma, Italy.

E-mail addresses: massimiliano.tognolini@unipr.it (M. Tognolini), alessio.lodola@unipr.it (A. Lodola).

ephrin-binding pocket of Eph receptors with potencies approaching the nanomolar range [10], or smaller synthetic peptides with micromolar potency [11,12]. Most of these peptides suffer from a significant proteolytic degradation *in vivo*, albeit chemical modifications allowed to improve their metabolic stability in rat plasma [13].

In the last years, small molecules able to disrupt the Eph–ephrin complex have been reported in the literature [14]. Most of these compounds demonstrated to exert their pharmacological activity by targeting the ligand-binding domain of the Eph receptor and thus to act as classical protein–protein interaction (PPI) inhibitors [15]. Among them, derivatives of lithocholic acid (compound **1**, Fig. 1) were discovered as competitive and reversible antagonists of the EphA2 receptor [16], active in prostate cancer [17] and cardiac muscle cells [18] at non-cytotoxic concentration. Other small molecules interfering with the Eph–ephrin system reported so far include i) 4-(2,5-dimethyl-1H-pyrrol-1-yl)-2-hydroxybenzoic acid (also known as CPD-1, Fig. 1) which is inactive by itself, but able to inhibit EphA2 and EphA4 after exposure to air and light [19]; ii) the farnesoid X receptor (FXR) agonist GW4064 [20], targeting EphA2 both in binding and functional assays [21]; and iii) the α 1-adrenoreceptor antagonist doxazosin, a micromolar binder of the EphA2 receptor able to reduce metastasis in mice [22].

Starting from lithocholic acid (**1**), we recently prepared a set of conjugates with amino acids able to interfere with the EphA2–ephrin-A1 interaction with potency in the micromolar range [23].

Two compounds emerged as the most promising EphA2 antagonists: *N*-(3 α -hydroxy-5 β -cholan-24-oyl)-L-tryptophan (UniPR126, compound **2**, Fig. 1, [23]) and *N*-(3 α -hydroxy-5 β -cholan-24-oyl)-L- β -homotryptophan (UniPR129, compound **3**, Fig. 1, [24]). They exhibited low micromolar inhibitory activity on EphA2 and were able to suppress angiogenesis in human umbilical vein endothelial cells (HUVECs). However, the usefulness of conjugates **2** and **3** as Eph–ephrin antagonists has been so far restricted to *in vitro* investigations, as these compounds suffer from poor physicochemical properties and limited selectivity [25], due to their lithocholic acid moiety.

To search for novel EphA2 antagonists, we recently applied a combined ligand- and structure-based virtual screening approach on a library of commercially available compounds, to select a set of lipophilic carboxylic acids that could serve as bioisostere analogues of lithocholic acid [26]. Among the selected compounds, the 3 β -hydroxy- Δ^5 -cholenic acid **4** was identified as a micromolar inhibitor of the EphA2–ephrin-A1 interaction with a pIC₅₀ of 4.40. While compound **4** was only barely more active than **1** (pIC₅₀ = 4.25), it did not activate most of the physiological targets of **1**, such as the nuclear receptors FXR and the pregnane X receptor (PXR) [27].

Despite the similar activity on EphA2 and the high 2-D similarity of lithocholic acid **1** and 3 β -hydroxy- Δ^5 -cholenic acid **4**, these two compounds significantly differ in the shape of their rigid core (Fig. 2). Compound **1** possesses a bent shape due to a *cis*-junction connecting ring A and B (steroidal nomenclature), while Δ^5 -

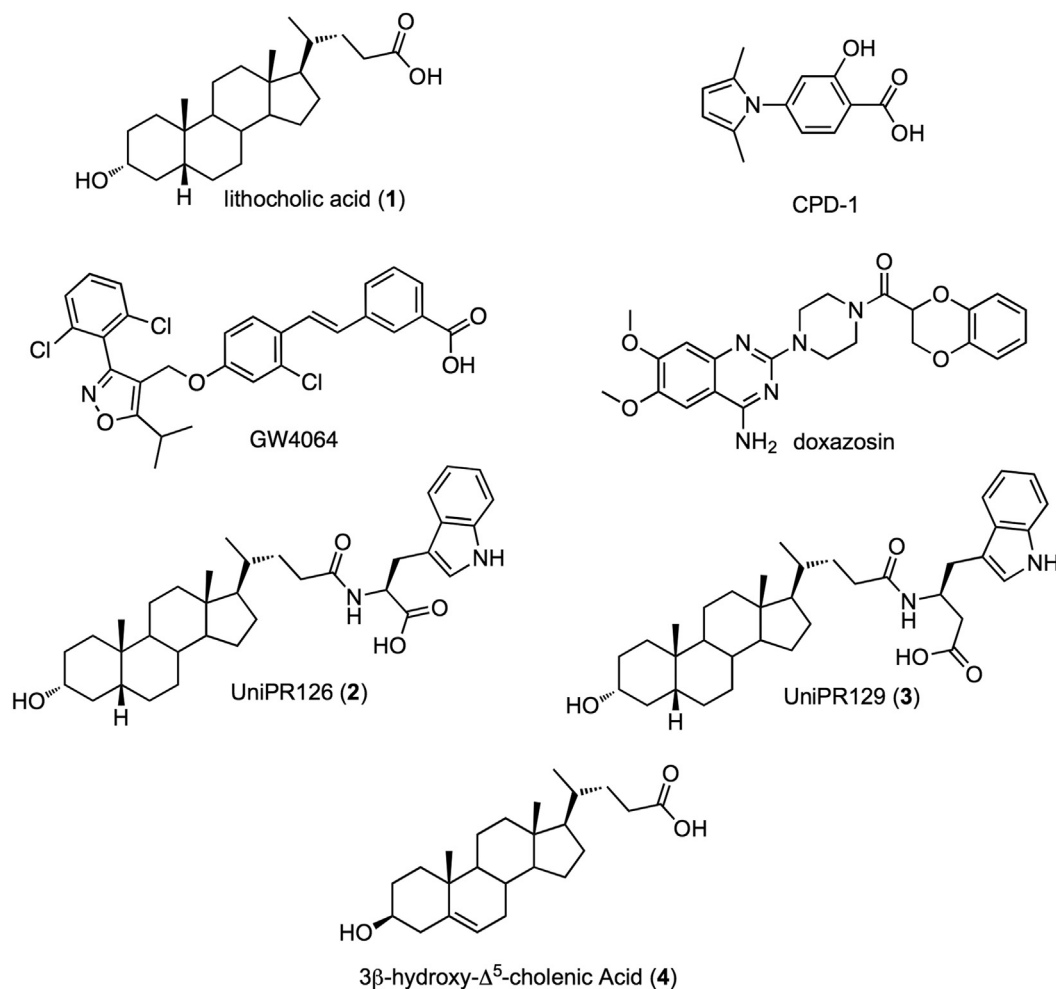


Fig. 1. Chemical structures of selected antagonists of the Eph–ephrin system.

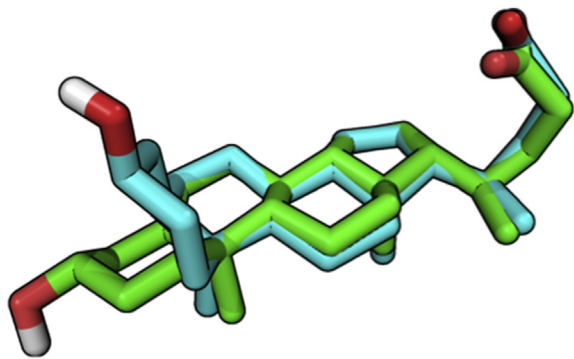


Fig. 2. Superposition of 3 β -hydroxy- Δ^5 -cholenic acid **4** (green carbon atoms) on lithocholic acid **1** (cyan carbon atoms) in their minimum energy conformation. (For interpretation of the references to color in this figure caption, the reader is referred to the web version of this article.)

cholenic acid **4** has an extended cholesterol-like structure arising from the sp^2 hybridization of the C5 and C6 carbon atoms.

We also evaluated whether **1** and **4** could adopt a similar binding mode within the EphA2 receptor by means of docking simulations [26]. These studies suggested that these two compounds, while being able to mimic the G-H loop of ephrin-A1 (i.e. the natural agonist of EphA2), occupy different regions of the EphA2 receptor (Fig. 3). Specifically, the A ring of **1** points toward Phe156, whereas that of compound **4** interacts with Ile58 on β -strand D. On the other hand, the carboxylate group of both antagonists is able to engage a salt bridge with Arg103 of EphA2, suggesting that the SAR profile previously collected for amino acid-conjugates of lithocholic acid should be transferable to Δ^5 -cholenic acid derivatives.

The modeled binding mode thus suggests that it would be possible to identify effective EphA2 antagonists by conjugating the carboxylic acid of 3 β -hydroxy- Δ^5 -cholenic acid with a panel of various amino acids. Moving from these premises, we report here the design, synthesis and pharmacological characterization of a series of amino acid conjugates of **4**. The synthesized compounds

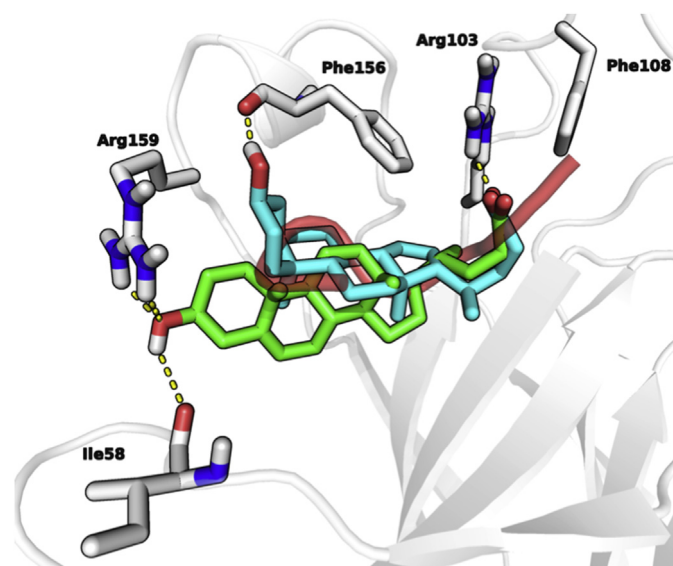


Fig. 3. 3 β -hydroxy- Δ^5 -cholenic acid **4** (green carbon atoms) and lithocholic acid **1** (cyan carbon atoms) in their docked conformation within the EphA2 receptor (white ribbons and white carbon atoms). The G-H loop of crystallized ephrin-A1 is depicted in red. (For interpretation of the references to color in this figure caption, the reader is referred to the web version of this article.)

were examined for their ability to i) prevent binding of biotinylated-ephrin-A1 to EphA2 receptor, ii) inhibit EphA2 phosphorylation in prostate cancer cells, iii) block angiogenesis in HUVE cells, and iv) interact with known off-targets of bile acid-derived compounds.

2. Chemistry

Conjugates **5–17** and **19–21** were prepared condensing the carboxylic acid group of the commercially available 3 β -hydroxy- Δ^5 -cholenic acid **4** to the amino group of various natural and unnatural amino acids by means of activation with an uronium-salt-based condensing agent (*O*-(benzotriazol-1-yl)-*N,N,N',N'*-tertamethyluronium tetrafluoroborate, TBTU), as depicted in Scheme 1 [28]. This procedure allows the chemoselective coupling of various amino acids without the need for protecting groups, provided that a one-pot, two-step sequence is adopted. By exposure of a chilled solution of cholenic acid **4** in DMF to strictly one equivalent of TBTU, the activated *O*-benzotriazol-1-yl-ester **i** is formed. Without isolation of **i**, direct addition of the amino acid produces the conjugates **5–17**, and **19–21** in good yield, after brief aqueous work-up and silica gel column chromatography (see Supplementary data for details). Compound **18** was obtained by direct condensation of cholenic acid **4** with L-Trp methyl-ester hydrochloride, while **20** was derived from **10** by acetylation of the 3- β -hydroxyl group with excess acetic anhydride in pyridine.

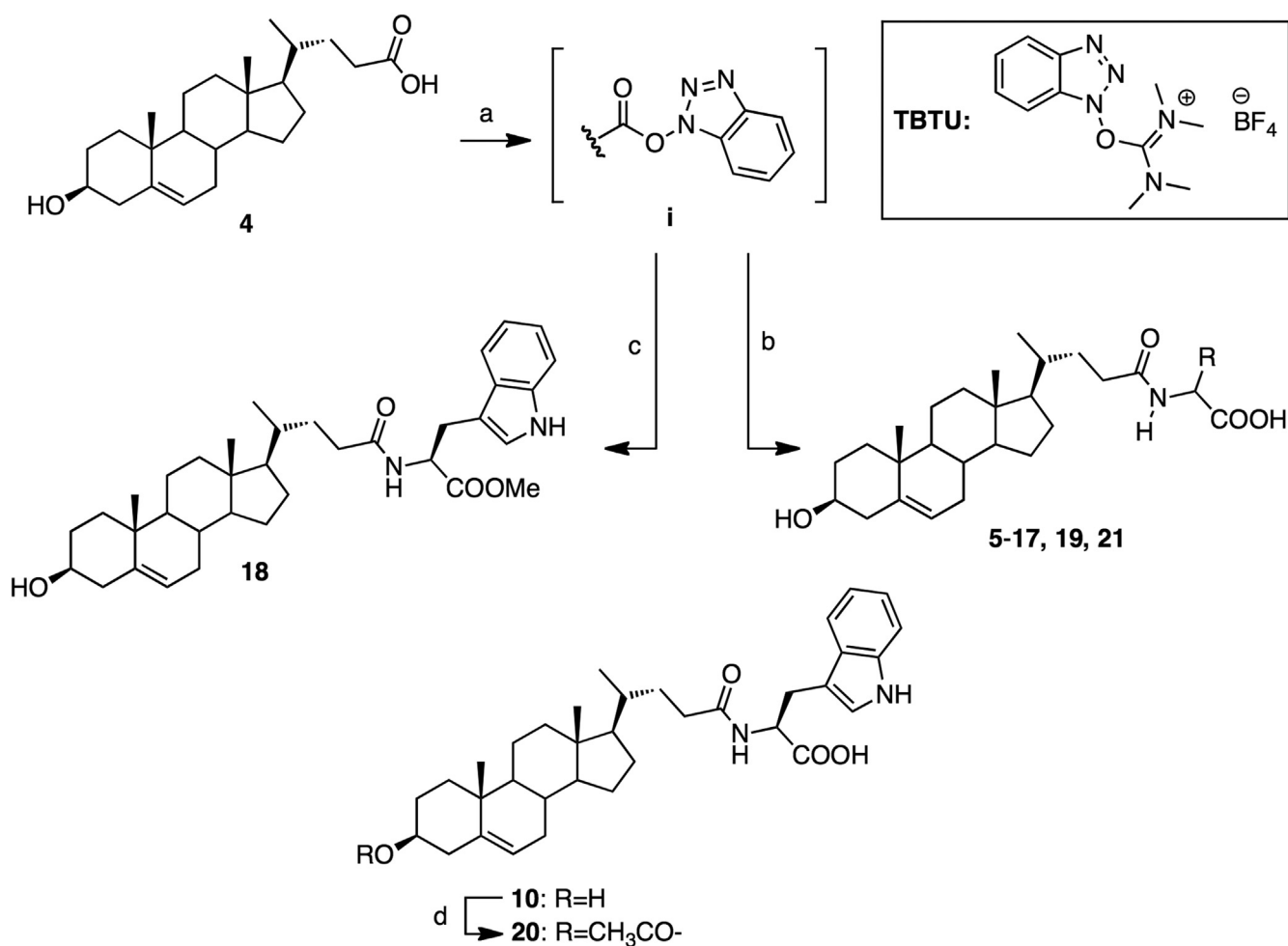
3. Results and discussion

3.1. Antagonism at the EphA2–ephrinA1 system and structure–activity relationships of 3 β -hydroxy- Δ^5 -cholenoyl amino acids

The synthesized compounds **5–21** were evaluated for their ability to disrupt the binding of biotinylated-ephrin-A1 to the EphA2 receptor, using a previously validated ELISA binding protocol [17]. The pIC_{50} values for the newly synthesized compounds are reported in Table 1, together with the corresponding standard error of the mean (SEM).

We began our structure–activity relationship (SAR) investigation by testing compounds **5–9** in which the 3 β -hydroxy- Δ^5 -cholenic acid nucleus was connected to α -amino acids of small (glycine, L-serine) or larger (L-methionine, L-phenylalanine, L-*O*-phenylserine) size. Unexpectedly, most of these compounds resulted inactive or weakly active at preventing the binding of ephrin-A1 to EphA2 receptor, regardless of their lipophilicity. Only the L-*O*-phenylserine derivative **9** retained an acceptable inhibitory activity displaying a pIC_{50} close to that of cholenic acid **4**. A noteworthy improvement in the potency was obtained conjugating **4** with L-tryptophan. The resulting *N*-(3 β -hydroxy- Δ^5 -cholen-24-oyl)-L-tryptophan (UniPR1331, **10**) was indeed ten times more potent than the parent compound **4** as it displayed a pIC_{50} of 5.45. Furthermore, the inhibitory potency of **10** was comparable to that of the analogue conjugate of lithocholic acid (i.e. compound **2**, Fig. 1, pIC_{50} = 5.69 [23]) corroborating the notion that 3 β -hydroxy- Δ^5 -cholenic acid is an effective bioisostere of lithocholic acid.

We next evaluated whether the improvement in the potency of **10** had to be ascribed to an *unspecific* increase in lipophilicity or to the formation of *specific* interactions within the EphA2 binding site. We thus prepared the D-Trp conjugate **11** and tested it in the ELISA assay. **11** resulted a weak inhibitor, displaying a detectable activity only at concentrations equal to or higher than 100 μ M, indicating that the indole nucleus of the L-tryptophan moiety is involved in specific interactions with the EphA2 receptor and can represent a starting point for a further SAR exploration. At first, we



Scheme 1. Reagents and conditions: a) DIPEA 2.2 eq, TBTU 1.0 eq, anh. DMF, 0 °C, 30 min; b) $\text{H}_2\text{N-CHR-COOH}$ (L-homo-Trp for **19**), 0 °C to rt, 16 h; c) L-Trp-OMe hydrochloride, 0 °C to rt, 16 h; d) $\text{Ac}_2\text{O/Pyridine}$ 1:1 v/v, rt, 16 h.

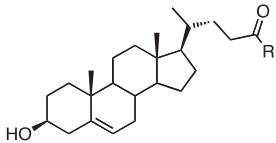

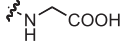
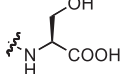
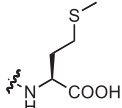
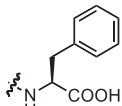
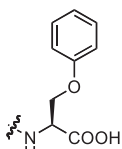
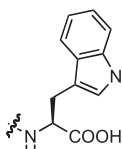
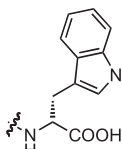
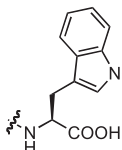
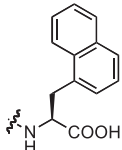
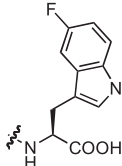
investigated if the indole $N\text{--H}$ group could establish polar interactions with EphA2. This proved not to be the case, as replacement of the hydrogen atom with a methyl group (compound **12**), did not affect the inhibitory potency ($\text{pIC}_{50} = 5.30$). This hypothesis was further corroborated by the $\alpha\text{-L-naphthylalanine}$ conjugate **13**, which possesses a pIC_{50} value of 5.39, very close to that of compounds **10** and **12**. Altogether, these data suggest that the increase in the pIC_{50} value of **10**, **12** and **13** compared to that of the parent compound **4** could be ascribed to their aromatic bicyclic nuclei, undertaking additional steric or electrostatic interactions within the EphA2 receptor. We then focused our attention on the indole ring of **10**, inserting in position 5 a balanced set of substituents featured by different electronic and steric properties (Fig. S1, supplementary data). Neither electron-withdrawing halogen groups ($-\text{F}$, **14** and $-\text{Br}$, **15**) nor electron-donating groups ($-\text{OH}$, **16** and $-\text{OCH}_3$, **17**) led to an increment in the inhibitory activity. Additionally, regardless of their electronic properties, only small substituents ($-\text{F}$, $-\text{OH}$) were tolerated. Conversely, the introduction in position 5 of bulkier substituents ($-\text{Br}$, $-\text{OCH}_3$) led to weaker inhibitors. This suggests that position 5 of the indole ring of L-Trp in compound **10** lies close to the EphA2 binding surface where only limited room is available to accommodate bulky substituents.

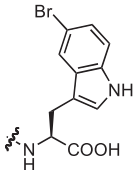
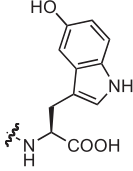
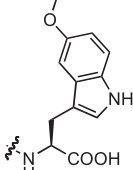
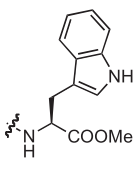
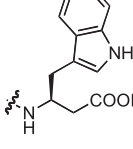
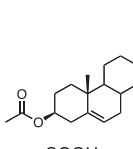
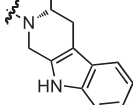
Finally, we investigated the role of the two terminal groups of **10** by modifying the carboxylic acid group of the tryptophan moiety and the 3β -hydroxyl group of the steroidal nucleus. While methyl-

ester **18** was inactive, compound **19**, the L-homo-Trp conjugate of **4** showed a pIC_{50} of 5.37, close to that of **10**, confirming the importance of a free carboxyl group. The 3β -hydroxyl substituent turned out to be an important structural element affecting the potency of these compounds, as the O -acetyl derivate **20** was thirty times less potent than the parent compound **10**.

We looked for a plausible binding mode for compound **10** by means of docking simulations with Glide software (see experimental section) employing the crystallographic coordinates of the EphA2 receptor in complex with its physiological ephrin-A1 ligand [29]. The top-ranked docking solution of compound **10** within EphA2 (pose A, $G_{\text{Score}} = -5.9$ kcal/mol) is reported in Fig. 4A. In this molecular model, compound **10** well fits the EphA2 binding channel, with its carboxylate group forming a salt bridge with Arg103 and the 3β -hydroxyl group undertaking H-bonds with Arg159 and Ile58. The accommodation of the L-Trp portion of **10** is consistent with the SAR data described above, as the benzene ring of the indole core interacts with Phe108 and Met73 while orienting its position 5 close to the EphA2 binding surface. Docking analysis identified an alternative binding mode for compound **10**, (pose B, $G_{\text{Score}} = -5.5$ kcal/mol, Fig. 4B) featured by a slightly worse docking score, but still consistent with the data reported in Table 1. This alternative pose B simply differs from the previous one for the accommodation of the indole ring, as the X_1 dihedral angle of the L-Trp moiety is about -180° , compared to the X_1 of -60° assumed in pose A (Fig. 4).

Table 1
pIC₅₀ values for compounds 5–21 tested on the EphA2–ephrin-A1 ELISA assay.

		
Cpd.	R	pIC ₅₀ ± SEM ^a
4		4.40 ± 0.12
5		Inactive ^b
6		<4.00
7		inactive ^b
8		<4.00
9		4.30 ± 0.09
10		5.45 ± 0.15
11		<4.00
12		5.30 ± 0.16
13		5.39 ± 0.15
14		5.05 ± 0.03

15		4.65 ± 0.10
16		5.22 ± 0.14
17		4.32 ± 0.07
18		Inactive ^b
19		5.37 ± 0.14
20		4.05 ± 0.06
21		5.20 ± 0.06

^a Values are means ± standard error of the mean (SEM) from at least three independent experiments.

^b No signal detected up to 100 μM.

To discriminate between the two possible orientations of the L-Trp side chain, we synthesized a conformationally constrained analogue of **10** by means of the Pictet–Spengler reaction [30], where the L-Trp moiety is forced to assume a X₁ value of –60° by means of a methylene group connecting position 2 of the indole nucleus to the α-nitrogen of the amino acid (Fig. 5). The inhibitory potency of the resulting compound **21** (pIC₅₀ = 5.20) closely matched that of **10**, supporting docking pose A as the putative binding mode for 3β-hydroxy-Δ⁵-cholenoyl L-Trp conjugates.

3.2. Pharmacological characterization of selected 3β-hydroxy-Δ⁵-cholenoyl L-Trp conjugates

To calculate the inhibitory constant (K_i) for the two most promising antagonists here identified, we built saturation curves (Fig. 6) relative to the ephrin-A1 binding to EphA2 in the presence

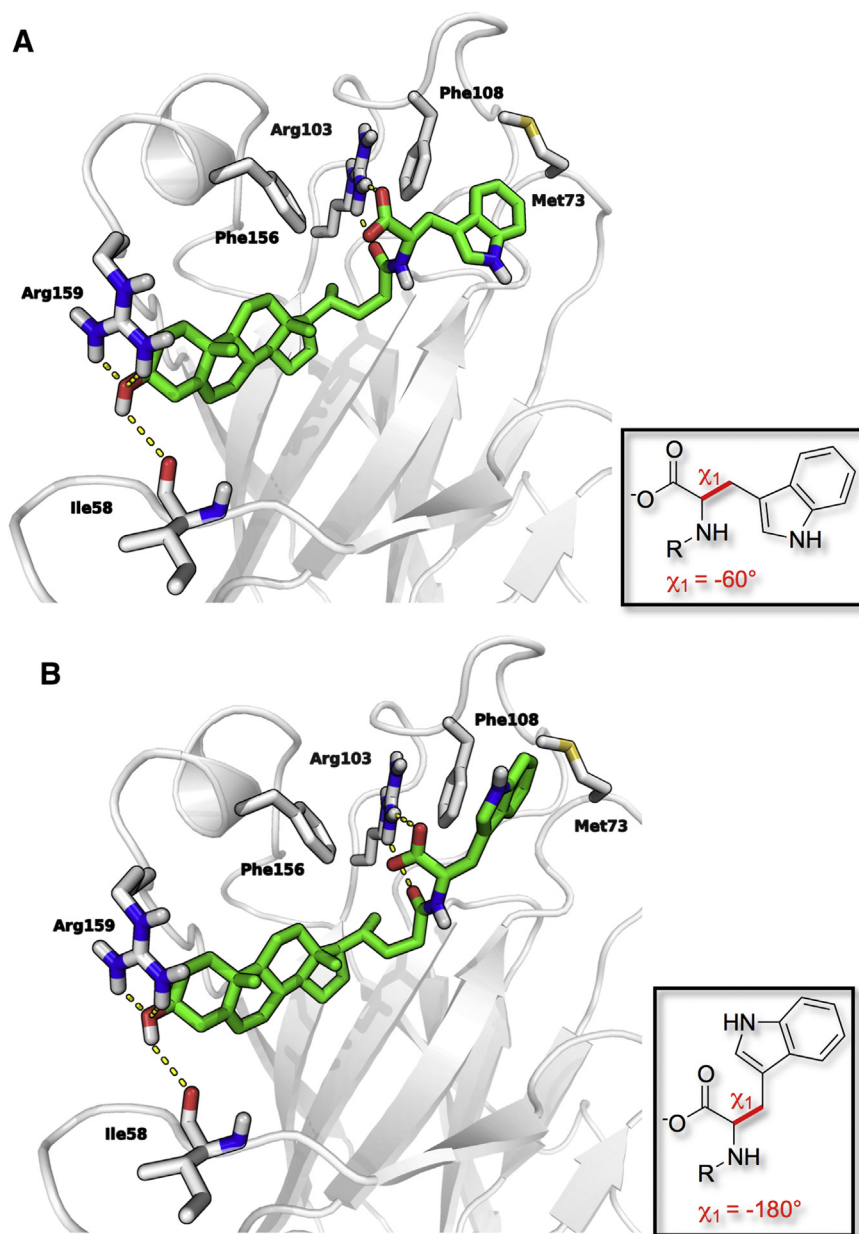


Fig. 4. Docking conformations of compound **10** (green carbons) within the binding site of EphA2 (white cartoons). Panel A, top-ranked pose, with a χ_1 dihedral angle of -60° for compound **10**. Panel B, alternative pose for **10**, with a χ_1 of -180° . (For interpretation of the references to color in this figure caption, the reader is referred to the web version of this article.)

of increasing concentrations of compound **10** (Fig. 6A) or **16** (Fig. 6C). For both compounds the curves appear to be surmountable and the Schild analysis [31] suggests that **10** (Fig. 6B) and **16** (Fig. 6D) act as competitive antagonists of the EphA2–ephrin-A1 system. The K_i values for **10** and **16** of 1.4 and 2.4 μM , respectively, are consistent with the pIC_{50} values reported in Table 1.

Further characterization of the binding properties of **10** was obtained using Surface Plasmon Resonance (SPR) technology [32]. The SPR analysis shows that **10** binds to the immobilized EphA2 receptor in a concentration-dependent manner (Fig. S2, supplementary data). The value of the steady-state affinity constant (K_D) of 3.3 μM , is consistent with the inhibitory constant obtained from the Schild analysis, suggesting that the ability of **10** to disrupt the EphA2–ephrin-A1 complex originates from a specific targeting of the EphA2 receptor.

3.3. Effects of selected 3β -hydroxy- Δ^5 -cholesterol L-Trp conjugates on EphA2 phosphorylation

To evaluate the biological properties of compounds **10** and **16** on the Eph–ephrin system, we performed phosphorylation studies in human prostate adenocarcinoma cells (PC3 line), which naturally express high levels of the EphA2 receptor [33]. These two compounds did not stimulate EphA2 phosphorylation (activation) on their own (data not shown), rather they inhibited EphA2 activation induced by ephrin-A1 in a concentration-dependent manner and with IC_{50} values of 9.3 μM and 13.9 μM for **10** and **16** respectively (Fig. 7). Crucially, compound concentrations which inhibited EphA2 phosphorylation were not cytotoxic on PC3 cells, confirming that the observed reduction in the phosphorylation levels was not due to a condition of cellular stress (Fig. S3, supplementary data).

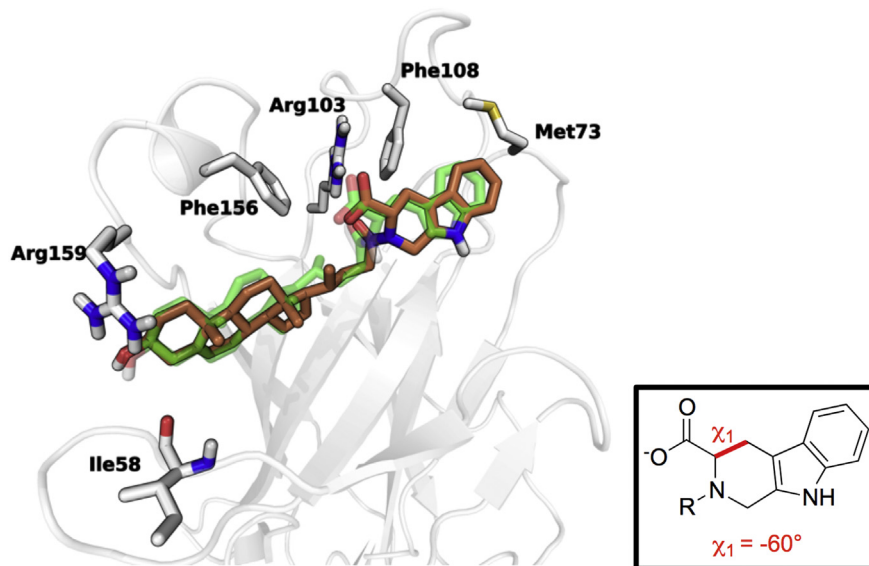


Fig. 5. Top-ranked docking pose for **21** (orange carbons) within the binding site of EphA2 (white cartoons). In this pose, the L-Trp moiety of **21** assumes a χ_1 value of -60° due to presence of methylene group connecting position 2 of the indole and the α -nitrogen of the amino acid. Compound **10** (shaded green carbon atoms) is reported for comparison in its docking pose A. (For interpretation of the references to color in this figure caption, the reader is referred to the web version of this article.)

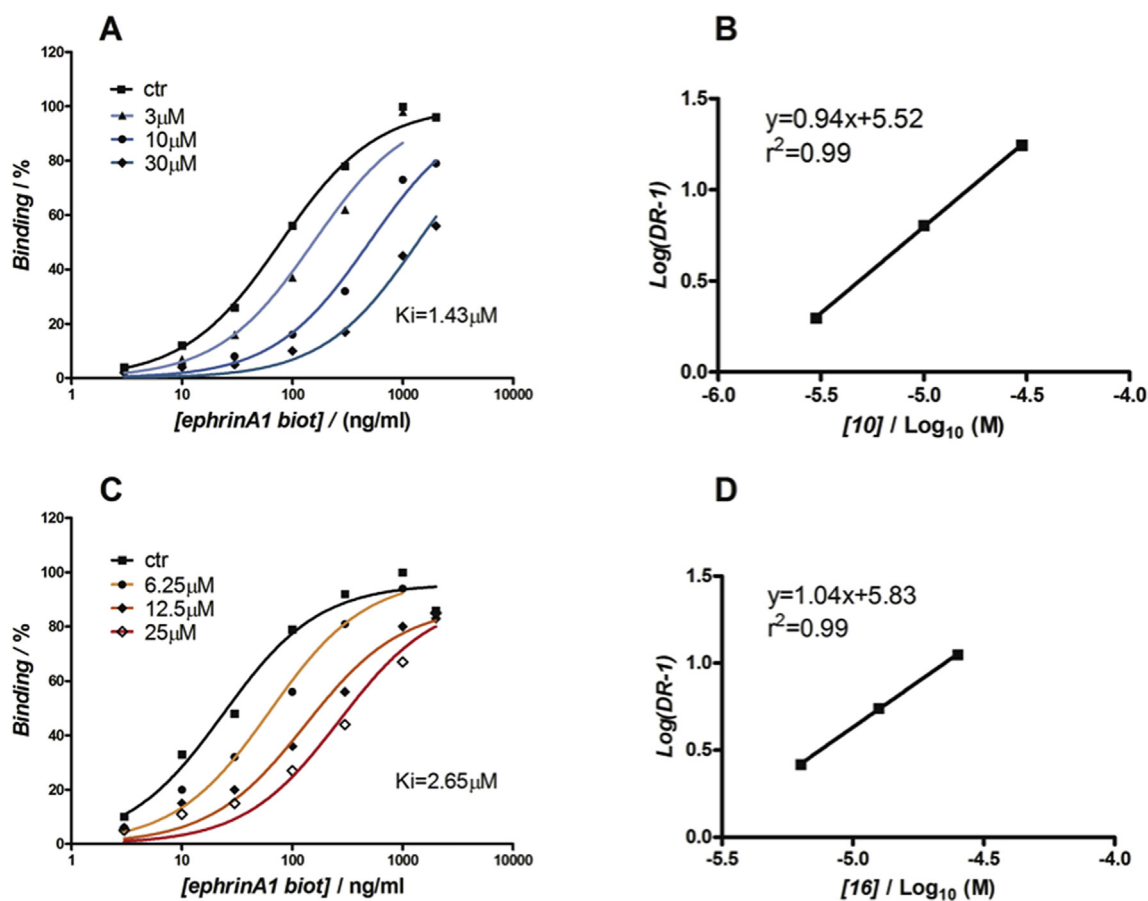


Fig. 6. Binding of biotinylated ephrin-A1 to immobilized EphA2-Fc in the presence of different concentrations of compound **10** (A, B) or **16** (C, D). Dissociation constants (K_D) from the previous experiments were used to calculate $\text{Log}(\text{dose-ratio} - 1)$ and to graph the Schild plot. The pK_i values were estimated by the intersection of the interpolated line with the X-axis.

We verified whether the ability of **10** to block EphA2 phosphorylation in cells was due to a direct interaction with its intracellular kinase domain. The catalytic activity of a recombinant

EphA2 kinase domain was monitored in presence of increasing concentrations of compound **10**. Evidence that compound **10** duly acts as genuine PPI inhibitor in intact cells came from the

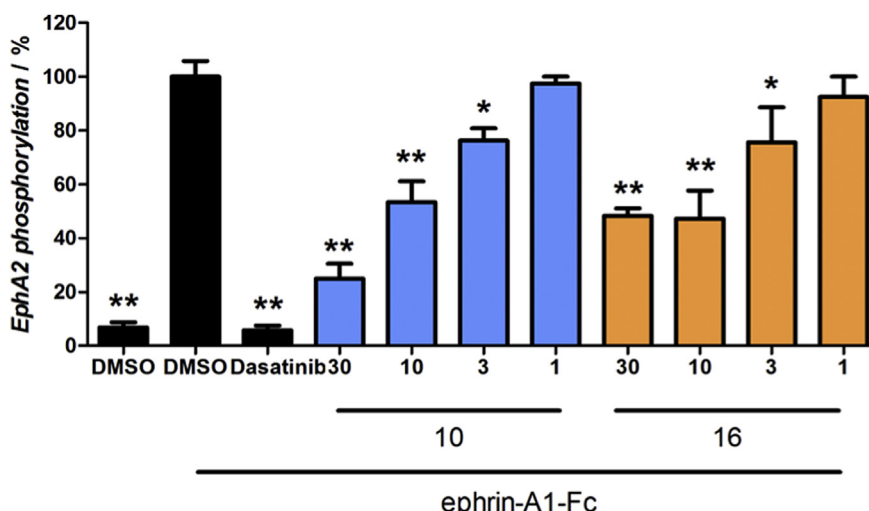


Fig. 7. Compound **10** or **16** blocks EphA2 activation induced by ephrin-A1 in PC3 cells. Cells were pretreated for 20 min with 1% DMSO, or the indicated concentrations (μM) of compounds, and then stimulated for 20 min with ephrin-A1-Fc (0.25 $\mu\text{g}/\text{ml}$). Phospho-EphA2 levels are relative to ephrin-A1-Fc + DMSO. Data are the means of three independent experiments \pm SEM. * $P < 0.05$, ** $P < 0.01$. Dasatinib (1 μM) was used as control for EphA2 inhibition in PC3 cells.

observation that it did not affect the enzyme activity up to 30 μM (Fig. 8). Conversely, the pan kinase inhibitor dasatinib, used as positive control for EphA2 inhibition [34], completely abolished EphA2 activity at 1 μM concentration.

3.4. Effects of compound 10 on angiogenesis

As the EphA2 receptor (along with EphB4) stimulates the formation of new vessels by endothelial cells [35], we evaluated if compound **10** was indeed able to interfere with angiogenic processes *in vitro*. We used a standard assay based on the differentiation of endothelial cells and the formation of tube-like structures on an extracellular matrix, i.e. Matrigel [36]. When HUVECs were incubated on Matrigel with compound **10**, we observed a dramatic reduction in the number of newly formed tubes compared to the control (Fig. 9).

A quantitative analysis demonstrated that compound **10** was able to reduce the formation of new tubes in a concentration-dependent manner, with an IC_{50} value of 2.9 μM , close to that of the reference Eph–ephrin antagonist **3** [24].

3.5. Selectivity profile of compound 10

We then set to examine the ability of **10** to inhibit the binding of

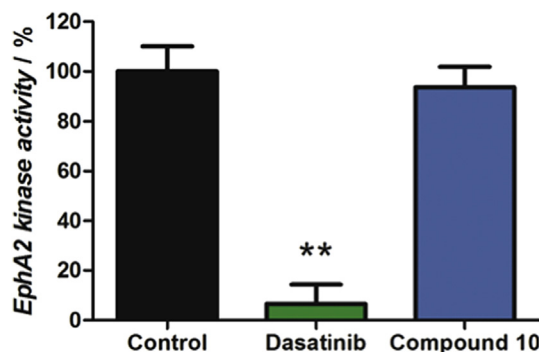


Fig. 8. Compound **10** (30 μM) does not inhibit enzymatic activity of the recombinant EphA2 kinase domain while Dasatinib (1 μM) fully abolish its activity. The activity of EphA2 was evaluated with an ELISA assay kit, incubating EphA2 with the indicated compound for 30 min.

ephrin-A1-Fc to EphA1–EphA8 receptors and the binding of ephrin-B1-Fc to EphB1–EphB6 receptors. Similarly to the other antagonists of the Eph–ephrin system (i.e. compounds **2** and **3** reported in Fig. 1) [23,24], **10** was able to inhibit ephrin binding to all members of the Eph receptor family with comparable inhibitory potency (Fig. 10). Considering the promiscuity of the Eph receptors in recognizing ephrin ligands, it is likely that the L-Trp derivative **10** binds to the conserved, high affinity region present in all the ligand-binding domain of the Eph receptors [37]. Relevant to this point, tumor progression is often a highly redundant process in which multiple receptors and signaling pathways contribute to an uncontrolled proliferation of cancer cells. As several ephrins and Eph receptor subtypes are co-expressed and biologically active in different solid tumors [38,39], the ability of **10** to block different Eph receptors might be exploited for the design and development of multi-target Eph receptor antagonists featured by a significant anti-tumor efficacy *in vivo*.

As anticipated, an additional selectivity issue of **10** is related to the presence of the steroidal nucleus. We sought to observe the potential interactions of **10** with privileged targets of steroidal derivatives, such as the G protein-coupled bile acid receptor 1 (GPBAR1, TGR5 [40]), a critical protein involved in glucose homeostasis [41], and the pregnane X receptor (PXR), which controls the expression of liver cytochromes [42]. The chenodeoxycholic acid derivative **10** did not activate TGR5 up to 30 μM , while the reference lithocholic acid derivative **3** was a rather potent agonist of this GPCR, showing a half maximal effective concentration (EC_{50}) value of 4.0 μM (Fig. S4, supplementary data). Likewise, **10** did not activate PXR up to 10 μM , while compound **3** had a small, but significant activating effect ($30 \pm 5\%$) on this receptor at the same concentration.

3.6. In vitro and in vivo pharmacokinetic (PK) properties of compound 10

We finally wondered if compound **10** was featured by higher systemic exposure in mice compared to Eph–ephrin antagonists derived from lithocholic acid i.e. compound **3** (UniPR129). After a single administration (30 mg/kg, os), the C_{max} of compound **10** at 30 min was 1.4 μM , one hundred times higher than the value observed for **3** ($C_{\text{max}} = 0.014 \mu\text{M}$) when administered at the same dose (Fig. 11). Additionally, the area under the curve (AUC_{0-t}), a

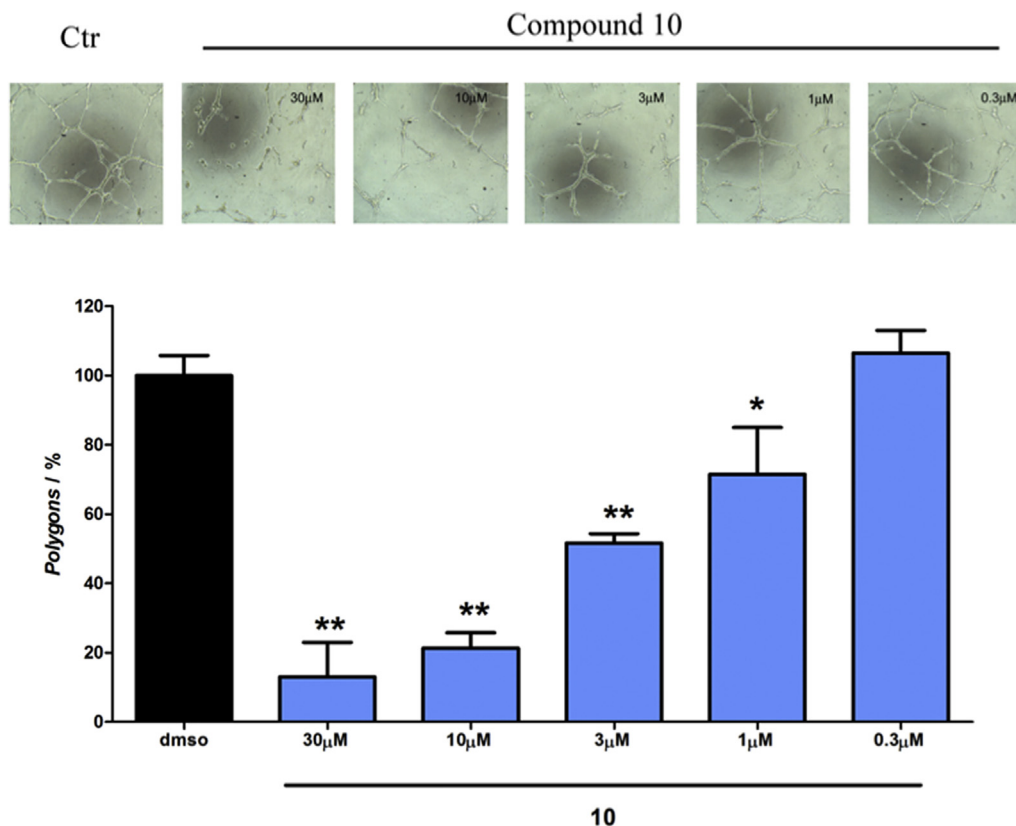


Fig. 9. Compound **10** inhibits *in vitro* angiogenesis in HUVECs. HUVECs seeded on Matrigel were treated with compound **10**, and images were taken 15 h later. The number of polygons is relative to 1% DMSO, which was used as the control. The histogram shows the means of at least three independent experiments \pm SEM. One-way ANOVA followed by Tukey's post-test was performed to compare the 1% DMSO control to all other conditions. * $P < 0.05$, ** $P < 0.01$.

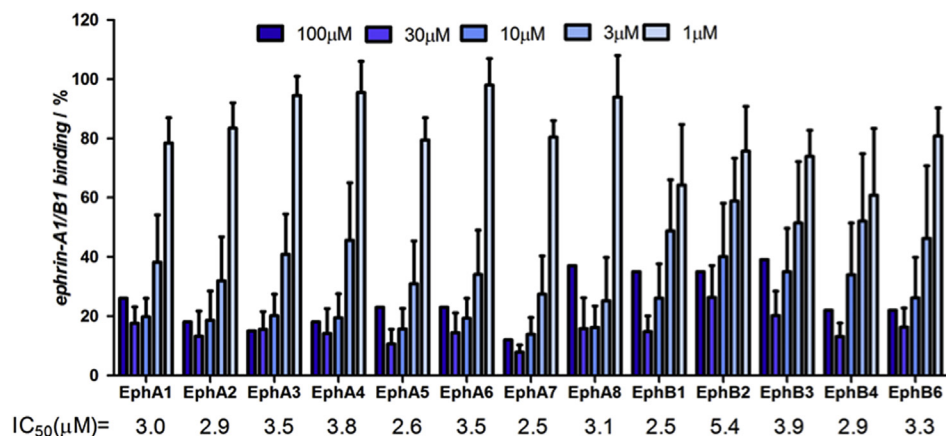


Fig. 10. Compound **10** is a pan-Eph receptor antagonist. Compound **10** dose-dependently inhibits binding of biotinylated ephrin-A1-Fc or ephrin-B1-Fc to EphA or EphB receptor ectodomains, respectively. Data are the means of at least three independent experiments \pm SEM. IC₅₀ values are indicated at the bottom.

measure of systemic exposure to the compound, was equal to 573.1 ng/mL h for **10**, significantly greater than that shown by compound **3** (AUC_{0-t} = 21.2 ng/mL h).

The significant difference in the systemic exposure between **10** and **3** prompted us to investigate if **10** was less prone than **3** to liver or plasmatic metabolism. We thus evaluated *in vitro* the metabolic stability of **10** and **3** by following their disappearance when incubated in murine plasma or liver S9 fraction. In both assays compounds **10** and **3** showed a similar stability (Table 2). In plasma, more than 95% of both compounds was recovered after

24 h of incubation indicating that the amide linkage of **3** and **10** was not significantly attacked by plasmatic hydrolytic enzymes. In mouse liver S9 fraction, one of the available model to investigate oxidative metabolism of xenobiotics [43] compounds **3** and **10** were recovered unmodified at a similar extent after 1 h of incubation, with percentage of remaining compound of 56 ± 5 for **3** and 70 ± 7 for **10**.

We thus looked at some of the physicochemical properties that may affect the oral absorption of a given compound. We thus measured the lipophilicity (i.e. the distribution coefficient in *n*-

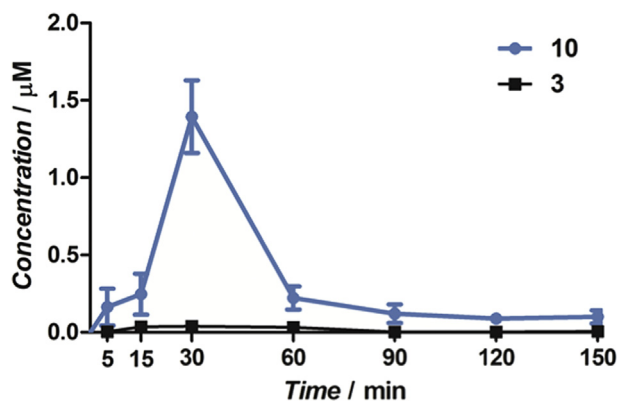


Fig. 11. Plasma profiles of compounds **10** (blue circles) and **3** (black squares). Plasma concentrations (μM) of the compounds over 150 min time course after a single administration in male mice (30 mg/kg, os) are reported as obtained from HPLC/MS analysis. Data are the means of at least three independent experiments \pm SEM. (For interpretation of the references to color in this figure caption, the reader is referred to the web version of this article.)

Table 2
Physicochemical and *in vitro* stability properties of compounds **3** and **10**.

Cpd	% Remaining compound in plasma ^a	% Remaining compound in liver ^b	$\log D_{\text{oct}, 7.4}$	Solubility ^c (μM)
3 (UniPR129)	98.3 \pm 9.5	56 \pm 5	4.90 \pm 0.15	31.8 \pm 4.2
10 (UniPR1331)	95.8 \pm 4.5	70 \pm 7	4.01 \pm 0.20	31.5 \pm 5.8

^a Percent remaining after 24 h of incubation, 37 °C.

^b Percent remaining after 1 h incubation in the presence of a NADPH-regenerating system in liver S9 fraction.

^c From DMSO stock solution. Data are the means of at least three independent experiments \pm SEM.

octanol/buffer at pH 7.4) and the kinetic solubility of compounds **3** and **10**. As indicated in Table 2, the cholenoyl derivative **10** resulted significantly less lipophilic than and as soluble as the lithocholic acid derivative **3**. We thus speculate that the higher oral bioavailability of **10** with respect to that of **3** might be due to a more favorable absorption phase helped by a lower log D value.

4. Conclusions

Two decades after its discovery, it is now widely accepted that the Eph–ephrin system has a pivotal function in tumor vascularization and carcinogenesis. In particular, the EphA2 and EphB4 receptors are currently being explored as potential targets for the development of anti-cancer therapies, with ongoing clinical trials based on the use of siRNA (EphA2, [44]) recombinant protein (EphB4, [45]) or pan-kinase inhibitor (i.e. with the XL647 compound targeting the kinase domain of EphB4, EGFR, and VEGFR2 [46]). On the other hand, drug discovery programs aimed at developing small molecule antagonists of the Eph–ephrin interaction are still in their infancy. Moreover, available antagonists of the Eph receptors suffer from severe chemical or pharmacological issues, which limit their use in animal models [47]. The most potent non-peptidic Eph antagonist reported so far (i.e. compound **3**), despite featuring a promising *in vitro* profile [24], failed to reach plasmatic concentrations suitable for *in vivo* experiments by oral route. In the present study we identified the *N*-(3 β -hydroxy- Δ^5 -cholen-24-oyl)-L-tryptophan **10** (UniPR1331) as a novel, promising Eph–ephrin antagonist with a more favorable PK profile than **3**. Compound **10** disrupts EphA2–ephrin-A1 interaction in the low

micromolar range and blocks *in vitro* angiogenesis at concentrations consistent with its binding affinity. Compound **10** overcomes specific key limitations of the lithocholic-based compound **3** being orally bioavailable in mice and devoid of interactions with off-targets relevant for compound **3**. We believe that **10** can represent a useful tool to evaluate the potential of pharmacological therapy based on small-molecule Eph receptor antagonists, and a starting point for the development of a new generation of orally available antagonists of the Eph–ephrin system.

5. Experimental section

5.1. Molecular modeling

5.1.1. Protein preparation

The crystal structure of the EphA2 receptor–ephrin-A1 complex (PDB ID: 3HEI [29]) was prepared for docking calculations with the Protein Preparation Wizard Tool [48], which added missing hydrogens and optimized the overall hydrogen bond network by adjusting the protonation state of aspartate, glutamate, lysine and histidine residues as well as the orientation of side chains of polar amino acids and of water molecules. The resulting all-atom structure was then submitted to a restrained minimization procedure with the OPLS 2005 force field [49] to a root-mean-square deviation of 0.3 Å calculated on heavy atoms. Prior to docking simulations, the ephrin-A1 ligand and all the water molecules were removed.

5.1.2. Docking simulations

Docking studies were built with Glide 6.1 [50]. Docking grids were centered in the hydrophobic channel of the EphA2 receptor accommodating the so-called “G–H loop” of ephrin-A1, which is delimited by Met66, Arg103, Phe108, Phe156 and Arg159. Dimensions of enclosing and bounding boxes were set to 32 and 10 Å on each side, respectively, and van der Waals radii of protein atoms were not scaled during grid generation. The three-dimensional structure of compounds **10** and **21** were initially built in Maestro 9.6 [51] and then energy-minimized with MacroModel 10.2 [52] applying the OPLS 2005 force field to an energy gradient of 0.05 kJ/(mol Å). Docking simulations were performed with Glide 6.1 in Standard Precision mode, imposing a hydrogen bond constraint on the protonated side chain of Arg103. Twenty poses were collected for each compound and subsequently ranked according to their G_{Score} value.

5.2. Chemistry

General information and details for each synthesized compound are given in the Supplementary data. The final compounds **5–21** were characterized by ^1H - and ^{13}C - NMR analysis as well as by MS. The purity of each compound was assessed by HPLC/MS analysis and shown to be 95% or higher. ^1H - and ^{13}C - NMR spectra are also provided in the Supplementary data section. The preparation of each compound has been carried out using the same general procedure, explanatory for compound **10** (*N*-(3 β -hydroxy- Δ^5 -cholen-24-oyl)-L-tryptophan). To a stirred solution of cholenic acid (183.1 mg, 0.489 mmol) in DMF (5.0 mL) at 0 °C, DIPEA (*N,N*-diisopropyl-*N*-ethylamine, 200 μL , 1.15 mmol) is added. To the obtained suspension, TBTU (*O*-(benzotriazol-1-yl)-*N,N,N',N'*-tetramethyluronium tetrafluoroborate, 195.2 mg, 0.515 mmol) is added, and the mixture is stirred at 0 °C for additional 25 min, when a perfectly clear solution appears. L-Trp (100.9 mg, 0.494 mmol) is then added and the mixture is allowed reaching room temperature while stirring for a total of 16 h. The mixture is poured over AcOEt (50 mL) and extracted with 2% v/v aqueous

H₂SO₄ (50 mL). The aqueous layer is discarded, and the organic layer is washed with half-saturated brine and then brine. The organic phase is dried over Na₂SO₄ and evaporated under reduced pressure. The crude material thus obtained is purified by silica gel column chromatography eluting at first with a 5% solution of methanol in dichloromethane, then with a mixture of DCM:MeOH:AcOH = 95:5:0.5 v/v/v to furnish **10** (215.5 mg, 79%) as a white amorphous solid. R_t HPLC (C18 150 × 4.6 mm, 5 μm, 1 mL/min, λ = 254 nm, A:B = 7:3 (A: MeOH + 0.1% v/v HCOOH; B: H₂O + 0.1% HCOOH v/v): 11.95 min; m.p.: 204–207 °C (dec.); ¹H NMR (CDCl₃/CD₃OD = 1:1, 400 MHz) δ: 7.53 (d, 1H, *J* = 7.9 Hz), 7.33 (d, 1H, *J* = 8.1 Hz), 7.09 (dt, 1H, *J* = 0.9, 8.1 Hz), 7.04 (s, 1H), 7.01 (dt, 1H, *J* = 0.9, 7.9 Hz), 5.31 (d, 1H, *J* = 4.8 Hz), 3.45–3.38 (m, 1H), 3.37–3.33 (m, 1H), 3.21 (dd, 1H, *J* = 6.8, 14.8 Hz), 2.26–2.13 (m, 3H), 2.06–1.90 (m, 3H), 1.85–1.60 (m, 4H), 1.57–1.27 (m, 8H), 1.25–1.01 (m, 6H), 0.98 (s, 3H), 0.86 (d, 3H, *J* = 6.5 Hz) 0.63 (s, 3H); ¹³C NMR (CDCl₃/CD₃OD = 1:1, 100 MHz) δ: 175.8, 175.0, 141.7, 137.4, 128.5, 124.1, 122.2, 119.7, 119.0, 112.1, 110.3, 72.0, 57.6, 56.6, 54.1, 51.1, 43.1, 42.6, 40.6, 38.1, 37.3, 36.3, 33.8, 32.8, 32.7, 32.5, 31.9, 28.8, 28.1, 25.0, 21.8, 19.9, 18.8, 12.3; MS-ESI, calc. for C₃₅H₄₈N₂O₄: 560.36, found: 561.6 [M + H⁺].

5.3. Pharmacology

All culture media and supplements were purchased from Euroclone (Milan, Italy). Recombinant proteins and antibodies were from R&D systems. Cells were purchased from ECACC (Porton Down, UK). Leupeptin, aprotinin, NP40, MTT, tween20, BSA and salts for solutions were from Applichem (Darmstadt, Germany); analytical grade extraction solvents, bile acids, EDTA and sodium orthovanadate were from Sigma (St. Louis, MO, USA). Mouse plasma was obtained from male mice (Charles River Laboratories, Milan, Italy). Animals were housed, handled, and cared accordingly to the European Community Council Directive 2010/63/UE, in Italian regulations (DL 26/2014) and with local ethical committee guidelines for animal research. Pooled plasma was obtained by cardiac puncture, collected into heparinized tubes, centrifuged (1900 g, 4 °C, 10 min) and stored at –70 °C until use. Mouse liver S₉ fractions were obtained from the same mice, transcardially perfused with 20 mL ice-cold KCl 0.15 M. Livers were removed, weighted, sliced into small pieces, and homogenized on ice with an ice-cold phosphate-buffered saline (PBS) solution (0.01 M, pH 7.4, 20% w/v). The S₉ fraction was obtained by centrifugation (9000 g, 4 °C, 30 min) and stored at –70 °C until use. Protein content was quantified by the colorimetric Bicinchoninic Acid assay (Pierce, Rockford, IL, USA), employing bovine serum albumin (BSA) as standard.

5.3.1. ELISA assays and Ki/IC₅₀ determination on EphA2

ELISA assays were performed as previously described [23]. 96-well ELISA high binding plates (Costar #2592) were incubated overnight at 4 °C with 100 μL/well of 1 μg mL^{–1} EphA2-Fc (R&D 639-A2) diluted in sterile phosphate buffered saline (PBS, 0.2 g/L KCl, 8.0 g/L NaCl, 0.2 g L^{–1} KH₂PO₄, 1.15 g/L Na₂HPO₄, pH 7.4). Next day the wells were washed with washing buffer (PBS + 0.05% tween20, pH 7.5) and blocked with blocking solution (PBS + 0.5% BSA) for 1 h at 37 °C. Compounds were added to the wells at proper concentration in 1% DMSO and incubated at 37 °C for 1 h. Biotinylated ephrin-A1-Fc (R&D Systems BT602) was added at 37 °C for 4 h at its K_D value in displacement assays or in a range from 1 to 2000 ng/mL in saturation studies. Then wells were washed and incubated with 100 μL/well Streptavidin-HRP (Sigma S5512) for 20 min at room temperature, washed again and finally incubated at room temperature with 0.1 mg/mL tetramethylbenzidine (Sigma T2885) reconstituted in stable peroxide

buffer (11.3 g/L citric acid, 9.7 g/L sodium phosphate, pH 5.0) and 0.02% H₂O₂ (30% m/m in water), added immediately before use. The reaction was stopped with 3N HCl 100 μL/well and the absorbance was measured using an ELISA plate reader (Sunrise, TECAN, Switzerland) at 450 nm. IC₅₀ values were determined using one-site competition non-linear regression analysis with Prism software (GraphPad Software Inc.). Ki were calculated using Schild analysis. To assess the selectivity of compound **10**, all EphA (R&D Systems SMPK1) and EphB (R&D Systems SMPK2) receptors were incubated overnight similarly to EphA2 as previously described; biotinylated ephrin-A1-Fc or biotinylated ephrin-B1-Fc (R&D Systems BT473) at their K_D values were used towards EphAs or EphBs, respectively.

5.3.2. Phosphorylation of EphA2 in PC3 cells

EphA2 phosphorylation was measured in cell lysates using DuoSet[®] IC Sandwich ELISA (R&D Systems DYC4065) following manufacturer's protocol. Briefly, 96-well ELISA high binding plates (costar 2592) were incubated overnight with 100 μL/well of the specific capture antibody diluted in sterile PBS at the proper working concentrations. Next day the wells were washed and blocked for 1 h and 100 μL/well of lysates were added for 2 h. Then, wells were incubated with the specific detection antibody and the phosphorylation level was revealed utilizing a standard HRP format and tetra-methylbenzidine through a colorimetric reaction read at 450 nm. Each step was performed at room temperature and followed by washing each well.

5.3.3. Phosphorylation of the EphA2 kinase domain

The kinase activity of the EphA2 kinase domain (Millipore, 14-560) was evaluated with the EphA2 kinase assay/inhibitor assay kit from Abnova (KA0061). This screening kit uses a horseradish peroxidase coupled anti-phosphotyrosine monoclonal antibody as a reporter molecule in a 96-wells ELISA format. The manufacturer instructions were followed to perform the assay (http://www.abnova.com/protocol_pdf/KA0061.pdf).

5.3.4. In vitro angiogenesis

Twenty-four well tissue culture plates were coated with BD Matrigel (80 μL/well) and incubated for 30 min at 37 °C in order to form a thin layer of gel on the bottom of the wells. HUVEC were treated with compound **10** (or DMSO as control) and 3.2 × 10⁵ cells/well were seeded on Matrigel. After 15 h of incubation the cells were fixed with 3.7% formaldehyde for 15 min at room temperature. Photographs were taken through a digital camera mounted on a microscope and the number of polygons formed was counted. Data were normalized to control (100%).

5.4. Pharmacokinetic studies

5.4.1. Single dose pharmacokinetic study in mice

Compounds **10** and **3** were formulated in 0.5% methylcellulose (10/90 v/v) for the oral administration. Test compounds were orally dosed as a single esophageal gavage at 30 mg/kg to male mice. Each group consisted of three mice. Blood samples were collected via tail puncture at 6–8 time points in the following range: 5 min–6 h (oral route). Whole blood samples were centrifuged at 5000 rpm for 10 min, and the resulting plasma samples were stored at –20 °C pending analysis. Compounds **10** and **3** were dosed in mouse plasma by HPLC-ESI-MS/MS employing a Thermo Accela UHPLC gradient system coupled to a Thermo TSQ Quantum Access Max triple quadrupole mass spectrometer (Thermo Italia, Milan, Italy) equipped with a heated electrospray ionization (H-ESI) ion source. (see [Supplementary data](#) for details on the HPLC-ESI-MS/MS method) Xcalibur 2.1 software (Thermo Italia, Milan, Italy) was

used for sample injection, peaks integration, and plasma level quantification.

5.4.2. Solubility measurements

Stock solutions (5 mM) of each compound were freshly prepared in DMSO. In a 96-well plate, a 2 mL aliquot of DMSO stock solution was added to 198 mL of 0.9% w/v NaCl solution. Plates were left into agitation (300 rpm) for 2 h at 25 °C. At the end of the incubation period, samples were centrifuged (16,000 g, 10 min, 20 °C) and the supernatant was diluted with an equal volume of methanol containing the Internal Standard **2** and injected in the HPLC-ESI-MS/MS system. The dissolved concentration was quantified by means of calibration curves built by serial dilution of stock solutions in MeOH.

5.4.3. LogD_{Oct, 7.4} measurements

Distribution coefficients (D) at physiological pH were measured by the shake-flask method at room temperature (21.0 ± 0.5 °C), employing the biphasic solvent system n-octanol/50 mM MOPS buffer pH 7.4, 0.15 M KCl ionic strength, mutually saturated by overnight stirring. A weighed amount of compound was dissolved in water-saturated n-octanol, buffer was added and the sample was stirred for 4 h to reach partition equilibrium. Partition phases were centrifuged (9000 g, 10 min, 20 °C), separated, diluted with methanol and dosed in HPLC-ESI-MS/MS.

5.4.4. Metabolic stability assays

They were carried out as previously described [53]. Briefly, stock solutions of **10** and **3** were prepared in DMSO immediately before use. Pooled plasma (400 µL) was incubated with 10 mM Phosphate Buffered Saline (PBS) pH 7.4 (95 µL) and 5 µL of compound stock solution in DMSO (final DMSO concentration: 1%; final compound concentration: 1 µM). In liver S₉ fraction stability assays, aliquots (50 mL) of liver S₉ fraction were quickly thawed and incubated (5 min, 37 °C) with the NADPH-generating system (2 mM NADP⁺, 10 mM glucose-6-phosphate, 0.4 U mL⁻¹ glucose-6-phosphate dehydrogenase, 5 mM MgCl₂) in PBS pH 7.4. At the end of the incubation period, compound stock solution (5 µL, 100 µM) in DMSO was added (final DMSO concentration in samples: 1%; final compound concentration: 1 µM). At fixed time points, aliquots (50 µL) were withdrawn, added with two volumes of CH₃CN containing the Internal Standard **2** centrifuged at 16,000 g for 5 min at 4 °C, and analyzed by HPLC-ESI-MS/MS. The instrument responses (i.e., peak area ratios of test compound vs. internal standard) were referred to the zero time-point samples (considered as 100%) in order to determine the percentage of compound remaining.

Acknowledgments

This work was supported by Ministero dell'Università e della Ricerca, "Futuro in Ricerca" program (project code: RBFR10FXCP).

Appendix A. Supplementary data

Supplementary data related to this article can be found at <http://dx.doi.org/10.1016/j.ejmech.2015.08.048>.

References

- [1] J.P. Himanen, N. Saha, D.B. Nikolov, Cell-cell signaling via Eph receptors and ephrins, *Curr. Opin. Cell Biol.* 19 (2007) 534–542.
- [2] E.B. Pasquale, Eph-ephrin bidirectional signaling in physiology and disease, *Cell* 133 (2008) 38–52.
- [3] A.W. Boyd, P.F. Bartlett, M. Lackmann, Therapeutic targeting of Eph receptors and their ligands, *Nat. Rev. Drug Discov.* 13 (2014) 39–62.
- [4] E.B. Pasquale, Eph receptors and ephrins in cancer: bidirectional signalling and beyond, *Nat. Rev. Cancer* 10 (2010) 165–180.
- [5] C.N. Landen Jr., C. Lu, L.Y. Han, K.T. Coffman, E. Bruckheimer, J. Halder, L.S. Mangala, W.M. Merritt, Y.G. Lin, C. Gao, R. Schmandt, A.A. Kamat, Y. Li, P. Thaker, D.M. Gershenson, N.U. Parikh, G.E. Gallick, M.S. Kinch, A.K. Sood, Efficacy and antivasculature effects of EphA2 reduction with an agonistic antibody in ovarian cancer, *J. Natl. Cancer Inst.* 98 (2006) 1558–1570.
- [6] P. Dobrzanski, K. Hunter, S. Jones-Bolin, H. Chang, C. Robinson, S. Pritchard, H. Zhao, B. Ruggeri, Antiangiogenic and antitumor efficacy of EphA2 receptor antagonist, *Cancer Res.* 64 (2004) 910–919.
- [7] J. Wykosky, W. Debinski, The EphA2 receptor and ephrinA1 ligand in solid tumors: function and therapeutic targeting, *Mol. Cancer Res.* 6 (2008) 1795–1806.
- [8] S. Wang, W.J. Placzek, J.L. Stebbins, S. Mitra, R. Noberini, M. Koolpe, Z. Zhang, R. Dahl, E.B. Pasquale, M. Pellicchia, Novel targeted system to deliver chemotherapeutic drugs to EphA2-expressing cancer cells, *J. Med. Chem.* 55 (2012) 2427–2436.
- [9] M. Tandon, S.V. Vemula, S.K. Mittal, Emerging strategies for EphA2 receptor targeting for cancer therapeutics, *Expert Opin. Ther. Targets* 15 (2011) 31–51.
- [10] M. Koolpe, R. Burgess, M. Dail, E.B. Pasquale, EphB receptor-binding peptides identified by phage display enable design of an antagonist with ephrin-like affinity, *J. Biol. Chem.* 280 (2005) 17301–17311.
- [11] B. Wu, Z. Zhang, R. Noberini, E. Barile, M. Giulianotti, C. Pinilla, R.A. Houghten, E.B. Pasquale, M. Pellicchia, HTS by NMR of combinatorial libraries: a fragment-based approach to ligand discovery, *Chem. Biol.* 20 (2013) 19–33.
- [12] S. Duggineni, S. Mitra, R. Noberini, X. Han, N. Lin, Y. Xu, W. Tian, J. An, E.B. Pasquale, Z. Huang, Design, synthesis and characterization of novel small molecular inhibitors of ephrin-B2 binding to EphB4, *Biochem. Pharmacol.* 85 (2013) 507–513.
- [13] R. Noberini, S. Mitra, O. Salvucci, F. Valencia, S. Duggineni, N. Prigozhina, K. Wei, G. Tosato, Z. Huang, E.B. Pasquale, PEGylation potentiates the effectiveness of an antagonistic peptide that targets the EphB4 receptor with nanomolar affinity, *PLoS One* 6 (2011) e28611.
- [14] A. Barquilla, E.B. Pasquale, Eph receptors and ephrins: therapeutic opportunities, *Annu. Rev. Pharmacol. Toxicol.* 55 (2015) 465–487.
- [15] M. Tognolini, I. Hassan-Mohamed, C. Giorgio, I. Zanotti, A. Lodola, Therapeutic perspectives of Eph-ephrin system modulation, *Drug Discov. Today* 19 (2014) 661–669.
- [16] M. Tognolini, M. Incerti, I. Hassan-Mohamed, C. Giorgio, S. Russo, R. Bruni, B. Lelli, L. Bracci, R. Noberini, E.B. Pasquale, E. Barocelli, P. Vicini, M. Mor, A. Lodola, Structure-activity relationships and mechanism of action of Eph-ephrin antagonists: interaction of cholanolic acid with the EphA2 receptor, *Chem. Med. Chem.* 7 (2012) 1071–1083.
- [17] C. Giorgio, I. Hassan Mohamed, L. Flammini, E. Barocelli, M. Incerti, A. Lodola, M. Tognolini, Lithocholic acid is an Eph-ephrin ligand interfering with Eph-kinase activation, *PLoS One* 6 (2011) e18128.
- [18] J. Jehle, I. Staudacher, F. Wiedmann, P.A. Schweizer, R. Becker, H.A. Katus, D. Thomas, Regulation of HL-1 cardiomyocyte apoptosis by EphA2 receptor tyrosine kinase phosphorylation and protection by lithocholic acid, *Br. J. Pharmacol.* 167 (2012) 1563–1572.
- [19] a) R. Noberini, S.K. De, Z. Zhang, B. Wu, D. Raveendra-Panickar, V. Chen, J. Vazquez, H. Qin, J. Song, N.D. Cosford, M. Pellicchia, E.B. Pasquale, A disubstituted acid-furanyl derivative inhibits ephrin binding to a subset of Eph receptors, *Chem. Biol. Drug Des.* 78 (2011) 667–678; b) W. Zhu, M. Groh, J. Hauptenthal, R.W. Hartmann, A detective story in drug discovery: elucidation of a screening artifact reveals polymeric carboxylic acids as potent inhibitors of RNA polymerase, *Chem. Eur. J.* 19 (2013) 8397–8400; c) A. Lodola, M. Incerti, M. Tognolini, On the use of 2,5-Dimethyl-Pyrrol-1-yl-Benzoic acid derivatives as Eph-ephrin antagonists, *J. Virol.* 88 (2014) 12173.
- [20] P.R. Maloney, D.J. Parks, C.D. Haffner, A.M. Fivush, G. Chandra, K.D. Plunket, K.L. Creech, L.B. Moore, J.G. Wilson, M.C. Lewis, S.A. Jones, T.M. Willson, Identification of a chemical tool for the orphan nuclear receptor FXR, *J. Med. Chem.* 16 (2000) 2971–2974.
- [21] M. Tognolini, M. Incerti, D. Pala, S. Russo, R. Castelli, I. Hassan-Mohamed, C. Giorgio, A. Lodola, Target hopping as a useful tool for the identification of novel EphA2 protein-protein antagonists, *Chem. Med. Chem.* 9 (2014) 67–72.
- [22] A. Petty, E. Myshkin, H. Qin, H. Guo, H. Miao, G.P. Tochtrop, J.T. Hsieh, P. Page, L. Liu, D.J. Lindner, C. Acharya, A.D. Mackerell Jr., E. Ficker, J. Song, B. Wang, A small molecule agonist of EphA2 receptor tyrosine kinase inhibits tumor cell migration in vitro and prostate cancer metastasis in vivo, *PLoS One* 7 (2012) e42120.
- [23] M. Incerti, M. Tognolini, S. Russo, D. Pala, C. Giorgio, I. Hassan-Mohamed, R. Noberini, E.B. Pasquale, P. Vicini, S. Piersanti, S. Rivara, E. Barocelli, M. Mor, A. Lodola, Amino acid conjugates of lithocholic acid as antagonists of the EphA2 receptor, *J. Med. Chem.* 56 (2013) 2936–2947.
- [24] I. Hassan-Mohamed, C. Giorgio, M. Incerti, S. Russo, D. Pala, E.B. Pasquale, P. Vicini, E. Barocelli, S. Rivara, M. Mor, A. Lodola, M. Tognolini, UniPR129 is a competitive small molecule Eph-ephrin antagonist blocking in vitro angiogenesis at low micromolar concentrations, *Br. J. Pharmacol.* 171 (2014) 5195–5208.
- [25] S. Russo, M. Incerti, M. Tognolini, R. Castelli, D. Pala, I. Hassan-Mohamed, C. Giorgio, F. De Franco, A. Gioiello, P. Vicini, E. Barocelli, S. Rivara, M. Mor, A. Lodola, Synthesis and structure-activity relationships of amino acid conjugates of cholanolic acid as antagonists of the EphA2 receptor, *Molecules* 18 (2013) 13043–13060.

- [26] D. Pala, R. Castelli, M. Incerti, S. Russo, M. Tognolini, C. Giorgio, I. Hassan-Mohamed, I. Zanotti, F. Vacondio, S. Rivara, M. Mor, A. Lodola, Combining ligand- and structure-based approaches for the discovery of new inhibitors of the EphA2-ephrin-A1 interaction, *J. Chem. Inf. Model.* 54 (2014) 2621–2626.
- [27] A. Gioiello, B. Cerra, W. Zhang, G.P. Vallerini, G. Costantino, F.D. Franco, D. Passeri, R. Pellicciari, K.D. Setchell, Synthesis of atypical bile acids for use as investigative tools for the genetic defect of 3 β -hydroxy- Δ (5)-C27-steroid oxidoreductase deficiency, *J. Steroid. Biochem.* 144 (2014) 348–360.
- [28] A. El-Faham, F. Albericio, Peptide coupling reagents, more than a letter soup, *Chem. Rev.* 111 (2011) 6557–6602.
- [29] J.P. Himanen, Y. Goldgur, H. Miao, E. Myshkin, H. Guo, M. Buck, M. Nguyen, K.R. Rajashankar, B. Wang, D.B. Nikolov, Ligand recognition by A-class Eph receptors: crystal structures of the EphA2 ligand-binding domain and the EphA2/ephrin-A1 complex, *EMBO Rep.* 10 (2009) 722–728.
- [30] A. Brossi, A. Focella, S. Teitel, Alkaloids in mammalian tissues. 3. Condensation of L-tryptophan and L-5-hydroxytryptophan with formaldehyde and acetaldehyde, *J. Med. Chem.* 16 (1973) 418–420.
- [31] O. Arunlakshana, H.O. Schild, Some quantitative uses of drug antagonists, *Br. J. Pharmacol. Chemother.* 14 (1959) 48–58.
- [32] M. Rusnati, M. Presta, Angiogenic growth factors interactome and drug discovery: the contribution of surface plasmon resonance, *Cytokine. Growth Factor Rev.* 26 (2015) 293–310.
- [33] H. Miao, E. Burnett, M. Kinch, E. Simon, B. Wang, Activation of EphA2 kinase suppresses integrin function and causes focal-adhesion-kinase dephosphorylation, *Nat. Cell. Biol.* 2 (2000) 62–69.
- [34] Q. Chang, C. Jorgensen, T. Pawson, D.W. Hedley, Effects of dasatinib on EphA2 receptor tyrosine kinase activity and downstream signalling in pancreatic cancer, *Br. J. Cancer* 99 (2008) 1074–1082.
- [35] N. Cheng, D.M. Brantley, J. Chen, The ephrins and Eph receptors in angiogenesis, *Cytokine Growth Factor Rev.* 13 (2002) 75–85.
- [36] M.L. Ponce, Tube formation: an in vitro matrigel angiogenesis assay, *Methods Mol. Biol.* 467 (2009) 183–188.
- [37] J.P. Himanen, Ectodomain structures of Eph receptors, *Semin. Cell. Dev. Biol.* 23 (2012) 35–42.
- [38] F. Al-Ejeh, C. Offenhäuser, Y.C. Lim, B.W. Stringer, B.W. Day, A.W. Boyd, Eph family co-expression patterns define unique clusters predictive of cancer phenotype, *Growth. Factors* 32 (2014) 254–264.
- [39] R. Noberini, E. Rubio de la Torre, E.B. Pasquale, Profiling Eph receptor expression in cells and tissues: a targeted mass spectrometry approach, *Cell. Adh. Migr.* 6 (2012) 102–112.
- [40] Y. Kawamata, R. Fujii, M. Hosoya, M. Harada, H. Yoshida, M. Miwa, S. Fukusumi, Y. Habata, T. Itoh, Y. Shintani, S. Hinuma, Y. Fujisawa, M. Fujino, A G protein-coupled receptor responsive to bile acids, *J. Biol. Chem.* 278 (2003) 9435–9440.
- [41] C. Thomas, A. Gioiello, L. Noriega, A. Strehle, J. Oury, G. Rizzo, A. Macchiarulo, H. Yamamoto, C. Matak, M. Pruzanski, R. Pellicciari, J. Auwerx, K. Schoonjans, TGR5-mediated bile acid sensing controls glucose homeostasis, *Cell Metab.* 10 (2009) 167–177.
- [42] J.L. Staudinger, B. Goodwin, S.A. Jones, D. Hawkins-Brown, K.I. MacKenzie, A. LaTour, Y. Liu, C.D. Klaassen, K.K. Brown, J. Reinhard, T.M. Willson, B.H. Koller, S.A. Kliewer, The nuclear receptor PXR is a lithocholic acid sensor that protects against liver toxicity, *Proc. Natl. Acad. Sci. U. S. A.* 98 (2001) 3369–3374.
- [43] T. Walle, X. Wen, U.K. Walle, Improving metabolic stability of cancer chemoprotective polyphenols, *Expert. Opin. Drug Metab. Toxicol.* 3 (2007) 379–388.
- [44] G. Ozcan, B. Ozpolat, R.L. Coleman, A.K. Sood, G. Lopez-Berestein, Preclinical and clinical development of siRNA-based therapeutics, *Adv. Drug Deliv. Rev.* 87 (2015) 108–119.
- [45] NCT01642342, Recombinant Albumin Fusion Protein SEphB4-HSA in Treating Patients with Metastatic or Recurrent Solid Tumors. See www.clinicaltrials.gov (Last accessed on 15.02.15).
- [46] M.C. Pietanza, S.M. Gadgeel, A.M. Dowlati, T.J. Lynch, R. Salgia, K.M. Rowland Jr., M.S. Wertheim, K.A. Price, G.J. Riely, C.G. Azzoli, V.A. Miller, L.M. Krug, M.G. Kris, J.H. Beumer, M. Tonda, B. Mitchell, N.A. Rizvi, Phase II study of the multitargeted tyrosine kinase inhibitor XL647 in patients with non-small-cell lung cancer, *J. Thorac. Oncol.* 7 (2012) 856–865.
- [47] M. Tognolini, M. Incerti, A. Lodola, Are we using the right pharmacological tools to target EphA4? *ACS Chem. Neurosci.* 5 (2014) 1146–1147.
- [48] Schrödinger Suite, Protein Preparation Wizard; Epik version 2.6, Schrödinger, LLC, New York, NY, 2013. *Impact* version 6.1, Schrödinger, LLC, New York, NY, 2013; *Prime* version 3.4, Schrödinger, LLC, New York, NY, 2013.
- [49] J.L. Banks, H.S. Beard, Y. Cao, A.E. Cho, W. Damm, R. Farid, A.K. Felts, T.A. Halgren, D.T. Mainz, J.R. Maple, R. Murphy, D.M. Philipp, M.P. Repasky, L.Y. Zhang, B.J. Berne, R.A. Friesner, E. Gallicchio, R.M. Levy, Integrated modeling program, applied chemical theory (IMPACT), *J. Comput. Chem.* 26 (2005) 1752–1780.
- [50] *Glide*, Version 6.1, Schrödinger, LLC, New York, NY, 2013.
- [51] *Maestro*, Version 9.6, Schrödinger, LLC, New York, NY, 2013.
- [52] *MacroModel*, Version 10.2, Schrödinger, LLC, New York, NY, 2013.
- [53] F. Vacondio, C. Silva, A. Lodola, C. Carmi, S. Rivara, A. Duranti, A. Tontini, S. Sanchini, J.R. Clapper, D. Piomelli, G. Tarzia, M. Mor, Biphenyl-3-yl alkyl-carbamates as fatty acid amide hydrolase (FAAH) inhibitors: steric effects of N-alkyl chain on rat plasma and liver stability, *Eur. J. Med. Chem.* 46 (2011) 4466–4473.